

Published in final edited form as:

Calcif Tissue Int. 2009 August ; 85(2): 119–126. doi:10.1007/s00223-009-9252-8.

Lysyl Oxidase (*Lox*) Gene Deficiency Affects Osteoblastic Phenotype

N. Pischon, DMD, PhD¹, J. M. Mäki, PhD², P. Weissaupt, DMD, PhD¹, N. Heng, DMD, PhD¹, A. H. Palamakumbura, PhD³, P. N'Guessan, MD, MPH, PhD⁴, A. Ding⁵, R. Radlanski, DMD, PhD⁵, H. Renz, PhD⁵, T. A. L. J. J. Bronckers, PhD⁶, J. Myllyharju, PhD², A. Kielbassa, DMD, PhD¹, B. M. Kleber, DMD, PhD¹, J.-P. Bernimoulin, MD, DMD, PhD¹, and P.C. Trackman, PhD³

¹Dept. of Operative Dentistry and Periodontology, Charité - Universitätsmedizin Berlin, Germany

²Oulu Center for Cell-Matrix Research, Biocenter Oulu, Dept. of Medical Biochemistry and Molecular Biology, University of Oulu, Finland

³Dept. of Oral Biology and Periodontology, Goldman School of Dental Medicine, Boston University, Boston, USA

⁴Dept. of Infectious Diseases and Pulmonology, Charité - Universitätsmedizin Berlin, Germany

⁵Dept. of Experimental Dental Medicine, Charité - Universitätsmedizin Berlin, Germany

⁶Dept. of Oral Cell Biology, ACTA, Vrije Universiteit Amsterdam, The Netherlands

Abstract

Lysyl oxidase (LOX) catalyzes cross-linking of elastin and collagen, which is essential for structural integrity and function of bone tissue. The present study examined the role of *Lox* gene deficiency for the osteoblast phenotype in primary calvarial osteoblasts from E18.5 *Lox* knockout (*Lox*^{-/-}) and wild type (*wt*) (C57 BL/6) mice. Next to *Lox* gene depletion, mRNA expression of *Lox* isoforms, LOXL1-4, was significantly down-regulated in *Lox*^{-/-} bone tissue. A significant decrease of DNA synthesis of *Lox*^{-/-} osteoblasts compared to *wt* was found. Early stages of osteoblastic apoptosis studied by Annexin-V binding as well as later stages of DNA fragmentation were not affected. However, mineral nodule formation and osteoblastic differentiation were markedly decreased, as revealed by significant down-regulation of osteoblastic markers, type I collagen, BSP and Runx2/Cbfa1.

Keywords

Lysyl oxidase; LOXL1-4; Knockout; Osteoblast

Introduction

Type I collagen is the principal constituent of extracellular bone matrix and a crucial determinant for mechanical properties of bone tissue [1,2]. Posttranslational collagen modifications result in the formation of a mature functional matrix, which is essential for subsequent matrix mineralization [3-6]. Lysyl oxidase (protein-lysine 6-oxidase; LOX) is a copper-dependent enzyme that initiates cross-linking of collagen and elastin by catalyzing oxidative deamination of ϵ -amino groups of lysine and hydroxylysine residues [3,7]. Several

LOX isoforms, lysyl oxidase-like proteins 1-4 (LOXL1-4) have been identified [8-13] and amine oxidase activities of some of them have been demonstrated [14,15]. In bone tissue, pyridinolines and deoxypyridinolines are the primary cross-links of mature type I collagen which provide mechanical integrity, rigidity, and strength [16,17] and diminished LOX enzyme activity results in an increased risk of bone deformities and fractures [18,19].

Cells secrete 50 kDa pro-LOX which is then processed by procollagen C-proteinases in the extracellular region, resulting in 32 kDa mature LOX enzyme and its 18 kDa LOX propeptide [20]. LOX has been detected in the intracellular space [21-23] and it has been suggested to regulate gene transcription and to play a dominant role in stabilizing a normal cell phenotype [24-28]. In osteoblastic cells (MC3T3-E1), we have shown that LOX seems to be specifically regulated in the course of osteoblast cell differentiation and this regulation is required for normal collagen deposition [29]. A stage-dependent distribution of LOX in differentiating osteoblasts with co-localization with the nuclear region as well as with the tubular network was found, which could indicate a role of LOX in the regulation of osteoblast development [21].

A lack of *Lox* gene expression leads to perinatal lethality in mice [30,31]. *Lox* knockout mice (*Lox*^{-/-}) develop to term but die soon thereafter just before or at birth [30,31]. Due to defective collagen and elastin cross-linkage, they suffer from severe cardiovascular and pulmonary defects [30-32]. In the present study, we examined the effects of *Lox* gene deficiency on the skeletal phenotype and osteoblast development.

Material and methods

Histological analysis

For Alcian Blue and Alizarin Red staining, embryonic day (E) 18.5 *Lox*^{-/-} mice as well as *wt* mice (C57 BL/6) were removed from the uterus, fixed and stored in 70 % ethanol. Prior to staining, skin and eyes were removed and calcified tissues were stained with Alcian Blue (0.3 % Alcian blue 8GX (EMD Chemicals, Gibbstown, NJ, USA), 70 % ethanol) and Alizarin Red solution (0.1 % Alizarin Red S (Wako Chemicals, Richmond, VA, USA), 95 % ethanol, 1 volume glacial acetic acid, 17 volumes 70 % ethanol) for 3 days. Samples were placed in 1 % KOH for 24-72 h and then stored in 70 % glycerol.

Moreover, three-dimensional histological reconstruction of two heads of each genotype was performed. Samples were fixed and embedded paraffin sections were cut at 10 µm-thick serial sections using a rotary microtome (Model 2065 Microtome; Reichert-Jung, Heidelberg, Germany) in frontal plane. Hematoxylin-eosin sections were evaluated and every 8th section was photographed and scanned images were aligned. Calcified tissues using the contours of well characterized landmarks (i.e. skull base structures) were reconstructed by computer software (Analysis Software; SIS, Münster, Germany) [33].

Measurement of collagen fibril diameter

Tissues were fixed in Karnovsky solution (1% glutaraldehyde, 1% tannin in 0.2 M phosphate buffer, pH 7.4) and then post-fixed with 1% osmium tetroxide in 0.1 M phosphate buffer. The samples were rinsed, dehydrated and embedded in epon/araldite502 resin (Ted Pella, Redding, CA, USA). Sections of 30-50 nm were stained with uranyl acetate and lead citrate and the images were observed on a CM-12 transmission electron microscope (Philips Electron Optics, Eindhoven, The Netherlands). Images were recorded at × 35,000 on SO-163 electron image film (Eastman Kodak, Rochester, NY). 500 fibril diameters were measured in randomly chosen areas using Analysis Software (SIS, Münster, Germany).

Primary calvarial osteoblast cultures

Lox^{-/-} and *wt* calvariae were digested (0.2 % collagenase), minced and cultured in growth medium containing of α -MEM supplemented with 10 % FCS, 100 U/ml penicillin, 100 μ g/ml streptomycin and nonessential amino acids in 6-well plates as has been previously established [34,35]. In the present study, cells from each calvaria were cultured separately, because the genotype of each embryo was determined by Southern blotting at a later timepoint. First and second cell passages were used for the experiments.

BrdU incorporation

Primary osteoblasts were plated on 96-well plates and cultivated for up to 48 h at 37 °C in growth medium. DNA synthesis was assessed in monolayer cultures by colorimetric immunoassay (BrdU Roche, Basel, Switzerland) at 405 nm. The assay is based on measuring BrdU (5-Bromo-2'-deoxyuridine) incorporation following 2 h labeling into newly synthesized DNA of replicating cells, by ELISA.

Cell apoptosis

Rapid binding of annexin V to phosphatidyl serine was used for the early identification of cells undergoing apoptosis, as described previously [36]. Cells, plated on 24-well plates were serum-starved for 24 h and then grown in the presence and absence of 1 μ M staurosporine for 6 h, 16 h, and 24 h at 37 °C. Then, cells were incubated with FITC-labeled annexin V (1 μ g/ml) and PI (2 μ g/ml) for 15 min at 15-25 °C and analyzed by fluorescence microscopy. In addition, a photometric ELISA was applied for detection of cytoplasmatic histone-associated DNA fragments (mono- and oligonucleosomes) in apoptotic osteoblastic cells (Cell Death Detection ELISA, Roche, Basel, Switzerland) [37,38]. Osteoblasts were cultivated in the presence and absence of 1 μ M staurosporine for 6 h, 16 h and 24 h at 37 °C. Then, cells were washed, lysed for 30 min and centrifuged at 15000 rpm for 10 min. The supernatant was transferred into a streptavidin-precoated microtiter plate and incubated with the immunoreagent (anti-histone biotin, anti-DNA peroxidase) for 2 h. After washing, substrate solution was added and absorbance was determined at 405 nm.

Also, lactate dehydrogenase (LDH) release, as a marker of cell necrosis, was determined in the supernatants by colorimetric Cytotoxicity Detection Kit (Roche, Basel, Switzerland).

Mineral nodule formation

Osteoblast differentiation was induced by growth medium supplementation with 5 mM β -glycerophosphate and 50 μ g/ml ascorbic acid for up to 21 d. Mineralized cultures were fixed and stained with 2 % Alizarin Red (pH 4.0) for 20 min. For quantification, incorporated Alizarin Red stain was eluted with 10 % cetylpyridiniumchloride and optical density was measured at 562 nm using a spectrophotometer.

Quantitative real-time PCR

Total cellular RNA from calvariae of E 18.5 murine embryos was isolated (RNeasy Mini Kit, Qiagen, Hilden, Germany) according to the manufacturer's protocol and real-time PCR was performed using sequence specific primers and the ABI Prism 7000 Sequence detection system (Applied Biosystems, Lincoln, CA, USA). Specific primers for LOX (# Mm00495386_ml), LOXL1 (# Mm01145734_ml), LOXL2 (# Mm00804740_ml), LOXL3 (# Mm00442953_ml), LOXL4 (# Mm00446385_ml), for bone differentiation markers bone sialoprotein (BSP) (#Mm00492555_ml), COL1A1 (# Mm 00801666_g1) and Runx2/Cbfa1 (# Mm00501578_ml) and β -2 microglobulin (# Mm00437762_ml) were Taqman probes and were purchased from Applied Biosystems (Lincoln, CA, USA). β -2 microglobulin was used as internal control. The

mRNA expression relative to β -2 microglobulin was determined and the fold changes were calculated using the *wt* values as calibrator by means of $2^{-\Delta\Delta CT}$ method [39].

Statistical methods

Statistical analyses were performed using a statistical software package (SPSS for Windows, version 14.0, Chicago, IL, USA) Comparisons between data of *Lox^{-/-}* and *wt* were made using an unpaired Student's *t*-test assuming equal variances, and P values < 0.05 were considered statistically significant.

Results

Skeletal phenotype

Alcian blue and Alizarin Red staining of the *Lox^{-/-}* compared to the *wt* mice demonstrated normal morphology of calcified structures (Fig. 1). Three-dimensional reconstructions (Fig. 2) indicate normal development of nasal, alveolar as well as teeth-related structures in *Lox^{-/-}* mice. However, handling of *Lox^{-/-}* samples compared to *wt* revealed fragile tissues and high sensitivity to KOH maceration.

Decreased collagen fibril diameter

Data in Figure 3 demonstrate decreased collagen fibril diameters in *Lox^{-/-}* compared to *wt* bone tissues. Quantitative analyses showed that the mean fibril diameter significantly ($p < 0.001$) decreased from 34.06 ± 4.18 nm in *wt* to 31.01 ± 3.78 nm in *Lox^{-/-}*.

LOX mRNA expression

To establish that LOX gene expression is diminished in *Lox^{-/-}* calvarial bone tissue and to analyze mRNA expression of LOX isoforms (LOXL1-4) quantitative real-time PCR was performed. Figure 4 shows a significantly ($p < 0.05$) diminished mRNA expression of LOX and its isoforms in *Lox^{-/-}* compared to *wt*.

BrdU incorporation

Primary osteoblasts from *Lox^{-/-}* and *wt* calvariae were cultivated for up to 48 h. Figure 5 demonstrates a statistically significant ($p < 0.05$) decrease of BrdU incorporation in *Lox^{-/-}* osteoblasts compared to *wt*.

Apoptosis

Evaluation of cell apoptosis in *Lox^{-/-}* compared to *wt* are given in Figure 6. At 6 h, 16 h and 24 h, no differences in annexin-V binding on outward-facing phosphatidylserine or PI binding (a,b) as well as in the detection of cytoplasmic histone-associated DNA fragments were found (c). Also, in the presence of 1 μ M staurosporine, as potent inducer of cell apoptosis, no differences in annexin-V binding and DNA fragmentation were noted between *Lox^{-/-}* and *wt* osteoblasts (data not shown). To exclude non-specific annexin V binding and DNA fragmentation we measured LDH release in the supernatants, as a marker of cell necrosis (d). No differences were found between *Lox^{-/-}* and *wt* osteoblasts at any time point studied.

Analysis of mineral deposition

We next examined whether decreased cell proliferation in *Lox^{-/-}* cells affects later stages of osteoblast differentiation such as mineral nodule deposition. Significantly ($p < 0.05$) less Alizarin Red stain was eluted from primary *Lox^{-/-}* osteoblast cultures compared to *wt*, indicating less mineralized nodule formation in *Lox^{-/-}* cells at day 14 as well as at day 21 (Table 1).

Analysis of osteoblast differentiation markers

Osteoblasts undergo different phases of differentiation [40]. In accordance with decreased mineralized nodule formation observed in *Lox*^{-/-} osteoblasts, figure 7 shows a statistically significant ($p < 0.05$) decrease of COL1A1 as well as of BSP and Runx2/Cbfa1 mRNA expression compared to *wt*.

Discussion

Extracellular posttranslational modifications of fibrillar type I-III collagens by LOX are crucial for collagen cross-linkage and for the accumulation of a functional collagen matrix in bone tissue [3,5,7]. In the present study, besides normal morphology of calcified structures, significant changes in collagen fibril formation as well as altered osteoblast differentiation were found in *Lox*^{-/-} compared to *wt* mice.

A significantly diminished truncated and non-functional LOX mRNA expression was demonstrated in *Lox*^{-/-} samples. In other collagen producing cell types such as mouse fibroblasts and vascular smooth muscle cells isolated from *Lox*^{-/-} mice, lysyl oxidation itself has been reduced approximately by 80 % [32] and the overall amount of immature collagen cross-links have been reported to be reduced by 40 % in *Lox*^{-/-} embryos [31], thus indicating that LOX's role in cross-linking is essential and may be also be important in osteoblasts. Also, amine oxidase activities have been demonstrated for other LOX isoforms [14,15], thus indicating that multiple LOX isoforms may be involved in cross-linkage. The present data show that LOX and LOXL1 are clearly the prominent forms at the RNA level in bone tissue. In contrary, LOXL2 and LOXL3 showed only minor expression, which may suggest that they are less relevant in bone metabolism. In MC3T3-E1 cells, it was shown that LOX, LOXL1 and 4 were regulated in the course of osteoblasts differentiation whereas constituent expression of LOXL3 and no expression of LOXL2 were found [41]. It has been suggested that LOX isoforms may partly compensate for the lack of LOX [30], which may have contributed to the fact that normal bone morphology was found in *Lox*^{-/-} bone tissues by histological means. However, in the present study, in the absence of *Lox*, other genes including LOX isoforms, LOXL1-4, were significantly down-regulated as well, which may suggest regulatory interactions between different isoforms in bone tissue. Whether effects on osteoblast development seen in the present study are primarily due to *Lox* deficiency or to its isoforms, or a combination of both, is still unknown. Moreover, observed effects of *Lox* depletion on osteoblasts could also potentially depend on both changes in LOX enzyme activity, as well as on altered functions of LOX propeptide, as recently shown in other cell types [24,27,28].

The formation of covalent cross-links by enzymatic LOX activity are required for the formation of mature and insoluble collagen [3,5,7]. In the present study, significantly decreased collagen fiber diameters have been measured in *Lox*^{-/-} tissues, indicating impaired collagen matrix accumulation. A functional collagenous bone matrix may be critical for cell-cell and cell-matrix interactions affecting cell differentiation. Previous studies suggest that LOX plays an important role in osteoblastic differentiation [21,29,42,43]. The present study demonstrates for the first time that *Lox* gene deficiency affects the osteoblastic phenotype. DNA synthesis was significantly decreased in *Lox*^{-/-} osteoblasts compared to *wt* cells. From our previous data, it is known that LOX can be localized in the intracellular space and LOX has been suggested to regulate gene transcription [21,24,25,29]. LOX binds to intracellular cell components, in particular to the microtubular network [21], which is considered a prerequisite for development of a proper mitotic spindle apparatus and normal cell cycle progression [44]. Further studies will examine involved transcriptional control of observed effects of *Lox* depletion on cell division. In addition, the balance of osteoblast proliferation and apoptosis determines the size of the osteoblast population [45]. In the present study, decreased cell proliferation was

accompanied by normal regulation of apoptosis in *Lox*^{-/-} osteoblasts, suggesting an overall decrease of the size of osteoblast population.

Osteoblasts pass through phenotypic changes with distinct patterns of gene expression as they differentiate [40]. The present data indicate that *Lox* gene does not only influence early but also later stages of osteoblast differentiation as well, as decreased mineral nodule formation in *Lox*^{-/-} cultures was noted. In addition, to gain insights into molecular mechanisms associated with this inhibition, we determined the expression levels of osteoblast transcription factors and phenotypic markers of various stages of osteoblast differentiation. Our data show that early markers of osteoblast differentiation such as type I collagen as well as the marker of fully differentiated osteoblasts, BSP, were significantly down-regulated in bone tissue lacking *Lox* gene. Additionally, Runx2/cbfa1, a master transcription factor for the osteoblast lineage, which positively controls the expression of type I collagen and BSP [46], was significantly decreased. Altogether, inhibition of differentiation could be a consequence of inhibited cell proliferation. Besides, *Lox* depletion seems to directly affect osteoblast differentiation, as shown by down-regulation of the expression of osteoblastic differentiation markers, and thus can not completely be explained by diminished cell density.

Further studies are warranted to examine the interaction between enzymatic collagen cross-linkage and cellular effects as well as its effects on the formation of functional bone tissue. Based on the present data, we suspect that LOX promotes bone development through mechanisms in addition to its well established role in collagen cross-linking, and further studies are in progress to address novel mechanisms of action in normal developing osteoblast cultures.

Acknowledgments

We thank B. Danielowski and V. Kanitz for the technical support in the laboratory. This study has been supported by a grant DE140066 to P.T., grants 202469 from the Health Science Council and the S. Juselius Foundation to J. M., a research stipend from DFG GK-325-00 to P.M. and N.H. as well as by a short term research fellowship from EMBO, from COST, a habilitation stipend from the Charité - Universitätsmedizin Berlin and by a research grant from DFG PI 420/3 to N.P.

References

1. Boskey AL. Matrix protein and mineralization: An overview. *Conn Tissue Res* 1996;35:375–363.
2. Fratzl P, Gupta HS, Paschalis EP, Roschger P. Structure and mechanical quality of the collagen-mineral nano-composite in bone. *J Mater Chem* 2004;14:2115–2123.
3. Kagan H, Trackman P. Properties and function of lysyl oxidase. *Am J Respir Cell Mol Biol* 1991;5:206–210. [PubMed: 1680355]
4. Prockop D, Kivirikko K. Collagens: molecular biology, diseases, and potentials for therapy. *Ann Rev Biochem* 1995;64:403–434. [PubMed: 7574488]
5. Yamauchi, M. Collagen: The major matrix molecule in mineralized tissues. In: JJB, A.; Garner, S., editors. *Calcium and phosphorus in health and disease*. CRC Press; New York: 1996. p. 127-141.
6. Knott L, Bailey A. Collagen cross-links in mineralizing tissues: a review of their chemistry, function, and clinical relevance. *Bone* 1998;22:181–187. [PubMed: 9514209]
7. Kagan, H. Biology and Regulation of Extracellular Matrix: A Series. In: Mecham, RP., editor. *Regulation of Matrix Accumulation*. Vol. 1. Orlando: Academic Press; 1986. p. 321-398.
8. Mäki JM, Kivirikko KI. Cloning and characterization of a fourth human lysyl oxidase isoenzyme. *J Biochem* 2001;355:381–387.
9. Mäki JM, Tikkanen H, Kivirikko KI. Cloning and characterization of a fifth human lysyl oxidase isoenzyme: the third member of the lysyl oxidase-related subfamily with four scavenger receptor cysteine-rich domains. *Matrix Biol* 2001;20:493–496. [PubMed: 11691589]

10. Kenyon K, Modi WS, Contente S, Friedman RM. A novel human cDNA with a predicted protein similar to lysyl oxidase maps to chromosome 15q24-q25. *J Biol Chem* 1993;268:18435–18437. [PubMed: 7689553]
11. Ito H, Akiyama H, Iguchi H, Iyama K, Miyamoto M, Ohsawa K, et al. Molecular cloning and biological activity of a novel lysyl oxidase-related gene expressed in cartilage. *J Biol Chem* 2001;276:24023–24029. [PubMed: 11292829]
12. Jourdan-Le Saux C, Le Saux O, Donlon T, Boyd CD, Csiszar K. The human lysyl oxidase-related gene (LOXL2) maps between markers D8S280 and D8S278 on chromosome 8p21.2-p21.3. *Genomics* 1998;51:305–307. [PubMed: 9722957]
13. Huang Y, Dai J, Tang R, Zhao W, Zhou Z, Wang W, et al. Cloning and characterization of a human lysyl oxidase-like 3 gene (hLOXL3). *Matrix Biol* 2001;20:153–157. [PubMed: 11334717]
14. Borel A, Eichenberger D, Farjanel J, Kessler E, Gleyzal C, Hulmes DJ, et al. Lysyl oxidase-like protein from bovine aorta. Isolation and maturation to an active form by bone morphogenetic protein-1. *J Biol Chem* 2001;276:48944–48949. [PubMed: 11684696]
15. Kim MS, Kim SS, Jung ST, Park JY, Yoon HW, Ko J, et al. Expression and purification of enzymatically active forms of the human lysyl oxidase-like protein 4. *J Biol Chem* 2003;278:52071–52074. [PubMed: 14551188]
16. Knott L, Whitehead C, Fleming R, Bailey A. Biochemical changes in the collagenous matrix of osteoporotic avian bone. *J Biochem* 1995;310:1045–1051.
17. Eyre DR, Dickson IR, Van Ness K. Collagen crosslinking in human bone and articular cartilage: age-related changes in the content of mature hydroxypyridinium residues. *J Biochem* 1988;252:495–500.
18. Geiger BJ, Steenbock H, Parsons HT. Lathyrism in the rat. *J Nutri* 1933;6:427–442.
19. Shim H, Harris ZL. Genetic defects in copper metabolism. *J Nutr* 2003;133:1527S–1531S. [PubMed: 12730458]
20. Uzel M, Scott I, Babakhanlou-Chase H, Palamakumbura A, Pappano W, Hong H, et al. Multiple bone morphogenetic protein-1 related mammal metalloproteinases process pro-lysyl oxidase at the correct physiological site and control lysyl oxidase activation in mouse embryo fibroblast cultures. *J Biol Chem* 2001;276:22537–22543. [PubMed: 11313359]
21. Guo Y, Pischon N, Palamakumbura AH, Trackman P. Intracellular distribution of the lysyl oxidase propeptide in osteoblastic cells. *Am J Physiol Cell Physiol* 2007;292:2095–2102.
22. Nellaiappan K, Risitano A, Liu G, Nicklas G, Kagan H. Fully processed lysyl oxidase catalyst translocates from the extracellular space into nuclei of aortic smooth-muscle cells. *J Biol Chem* 2000;275:576–582.
23. Li W, Nellaiappan K, Strassmaier T, Graham L, Thomas K, Kagan H. Localization and activity of lysyl oxidase within nuclei of fibrogenic cells. *Proc Natl Acad Sci USA* 1997;94:12817–12822. [PubMed: 9371758]
24. Palamakumbura A, Jeay S, Guo Y, Pischon N, Sommer P, Sonenshein G, et al. The propeptide domain of lysyl oxidase induces phenotypic reversion of ras-transformed cells. *J Biol Chem* 2004;279:40593–40600. [PubMed: 15277520]
25. Jeay S, Pianetti S, Kagan H, S GE. Lysyl oxidase inhibits ras-mediated transformation by preventing activation of NF-kappa B. *Mol Cell Biol* 2003;23:2251–2263. [PubMed: 12640111]
26. Giampuzzi M, Oleggini R, Di Donato A. Demonstration of in vitro interaction between tumor suppressor lysyl oxidase and histones H1 and H2: definition of the regions involved. *Biochim et Biophys Acta* 2003;1647:245–251.
27. Min C, Kirsch KH, Zhao Y, Jeay S, Palamakumbura AH, Trackman PC, et al. The tumor suppressor activity of the lysyl oxidase propeptide reverses the invasive phenotype of Her-2/neu-driven breast cancer. *Cancer Res* 2007;67:1105–1112. [PubMed: 17283144]
28. Wu M, Min C, Wang X, Yu Z, Kirsch K, Trackman PC, et al. Repression of BCL2 by the tumor suppressor activity of the lysyl oxidase propeptide inhibits transformed phenotype of lung and pancreatic cancer cells. *Cancer Res* 2007;67:6278–6285. [PubMed: 17616686]
29. Hong HH, Pischon N, Santana RB, Palamakumbura AH, Chase HB, Gantz D, et al. A role for lysyl oxidase regulation in the control of normal collagen deposition in differentiating osteoblast cultures. *J Cell Physiol* 2004;200:53–62. [PubMed: 15137057]

30. Mäki JM, Räsänen J, Tikkanen H, Sormunen R, Mäkikallio K, Kivirikko KI, et al. Inactivation of the lysyl oxidase gene *Lox* leads to aortic aneurysms, cardiovascular dysfunction, and perinatal death in mice. *Circulation* 2002;106:2503–2509. [PubMed: 12417550]
31. Hornstra I, Birge S, Starcher B, Bailey A, Mecham R, Shapiro S. Lysyl oxidase is required for vascular and diaphragmatic development in mice. *J Biol Chem* 2003;278:14387–14393. [PubMed: 12473682]
32. Mäki J, Sormunen R, Lippo S, Kaarteenaho-Wiik R, Soininen R, Myllyharju J. Lysyl oxidase is essential for normal development and function of the respiratory system and for the integrity of elastic and collagen fibers in various tissues. *Am J Pathol* 2005;167:927–936. [PubMed: 16192629]
33. Radlanski RJ, Renz H, Klarkowski MC. Prenatal development of the human mandible. 3D reconstructions, morphometry and bone remodelling pattern, sizes 12–117 mm. *CRL Anat Embryol* 2003;207:221–232.
34. Bellows CG, Aubin JE, H JNM, Antosz ME. Mineralized bone nodules formed in vitro from enzymatically released rat calvaria cell populations. *Calcif Tissue Int* 1986;38:143–154. [PubMed: 3085892]
35. Ecarot-Charrier B, Glorieux FH, Van der Rest M, Pereira G. Osteoblasts isolated from mouse calvaria initiate matrix mineralization in culture. *J Cell Biol* 1983;96:639–643. [PubMed: 6833375]
36. Hippenstiel S, Schmeck B, N'Guessan PD, Seybold J, Krull M, Preissner K, et al. Rho protein inactivation induced apoptosis of cultured human endothelial cells. *Am J Physiol Lung Cell Mol Physiol* 2002;283:L830–838. [PubMed: 12225960]
37. N'Guessan PD, Vigelahn M, Bachmann S, Zabel S, Opitz B, Schmeck B, et al. The *UspA1* protein of *Moraxella catarrhalis* induces CEACAM-1-dependent apoptosis in alveolar epithelial cells. *J Infect Dis* 2007;195:1651–1660. [PubMed: 17471435]
38. N'Guessan PD, Schmeck B, Ayim A, Hocke AC, Brell B, Hammerschmidt S, et al. *Streptococcus pneumoniae* R6x induced p38 MAPK and JNK-mediated caspase-dependent apoptosis in human endothelial cells. *Thromb Haemost* 2005;94:295–303. [PubMed: 16113818]
39. Livak KJ, Schmittgen TD. Analysis of relative gene expression data using real-time quantitative PCR and the 2^{-ΔΔC_T} method. *Methods Enzymol* 2001;25:402–408.
40. Stein G, Lian J, Stein J, Van Wijnen J, Montecino M. Transcriptional control of osteoblast growth and differentiation. *Physiol Rev* 1996;76:593–629. [PubMed: 8618964]
41. Atsawasuwan P, Mochida Y, Parisuthiman D, Yamauchi M. Expression of lysyl oxidase isoforms in MC3T3-E1 osteoblastic cells. *Biochemical and Biophysical Research Communications* 2005;327:1042–1046. [PubMed: 15652501]
42. Pischon N, Darbois LM, Palamakumbura AH, Kessler E, Trackman PC. Regulation of collagen deposition and lysyl oxidase by tumor necrosis factor- α in osteoblasts. *J Biol Chem* 2004;279:30060–30065. [PubMed: 15138266]
43. Turecek C, Fratzl-Zelman N, Rumpler M, Buchinger B, Spitzer S, Zoehrer R, et al. Collagen cross-linking influences osteoblastic differentiation. *Calcif Tissue Int* 2008;82:392–400. [PubMed: 18488133]
44. Jordan MA. Mechanism of action of antitumor drugs that interacts with microtubules and tubulin. *Curr Med Chem Anti- Cancer Agents* 2002;2:1–17.
45. Hock JM, Krishnan V, Onyia JE, Bidwell JP, Milas j, Stanislaus D. Osteoblast apoptosis and bone turnover. *J Bone Mineral Res* 2001;16:975–984.
46. Ducy P, Zhang R, Geoffroy V, Ridall AL, Karsenty G. *Osf2/Cbfa1*: a transcriptional activator of osteoblast differentiation. *Cell* 1997;89:747–754. [PubMed: 9182762]

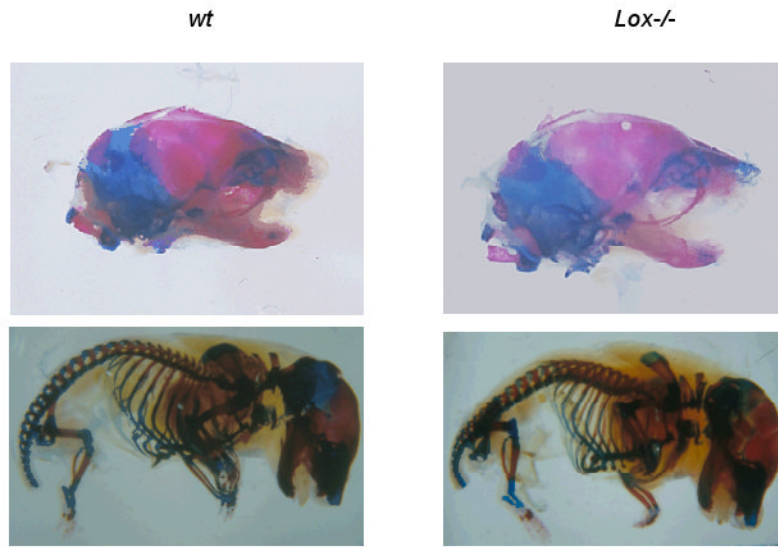


Figure 1. Lateral views of E 18.5 calcified tissues of *Lox^{-/-}* and *wt* mice stained with Alizarin Red and Alcian Blue. Experiments were performed three times. Representative images of one experiment are shown.

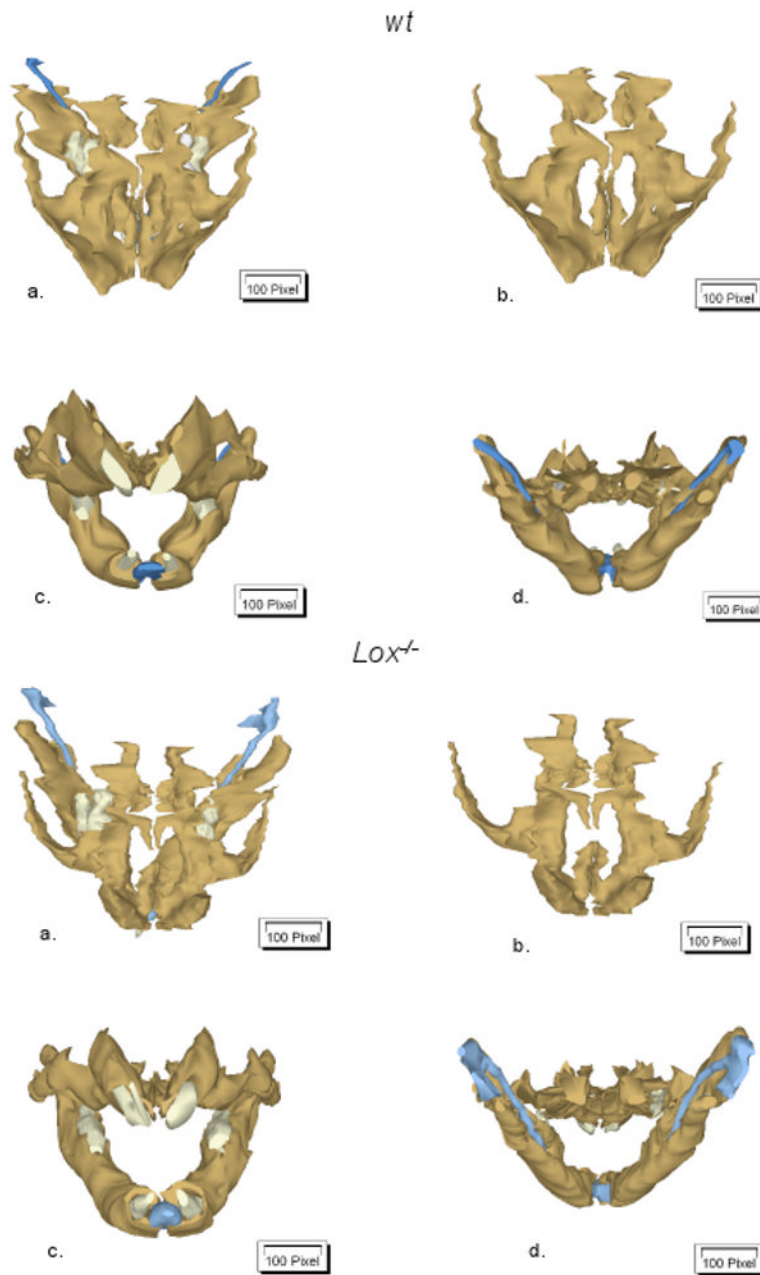


Figure 2.

Three-dimensional reconstructions of *Lox^{-/-}* and *wt* alveolar as well as of teeth-related structures. Reconstructions were performed two times for each genotype. Representative images (coronal (a-b), frontal (c) and dorsal (d) views) of one experiment are shown. Bone tissue is presented in brown, while Meckel's cartilage and teeth are given in blue and white colors, respectively.

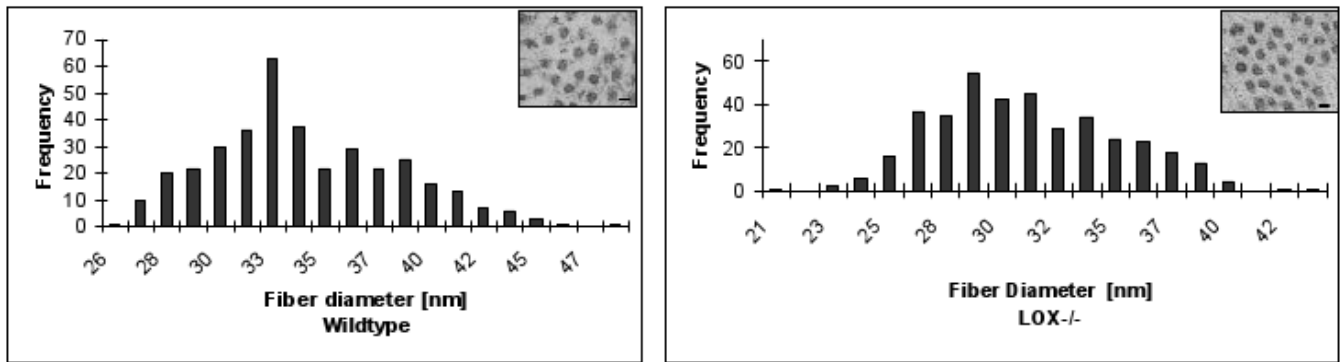
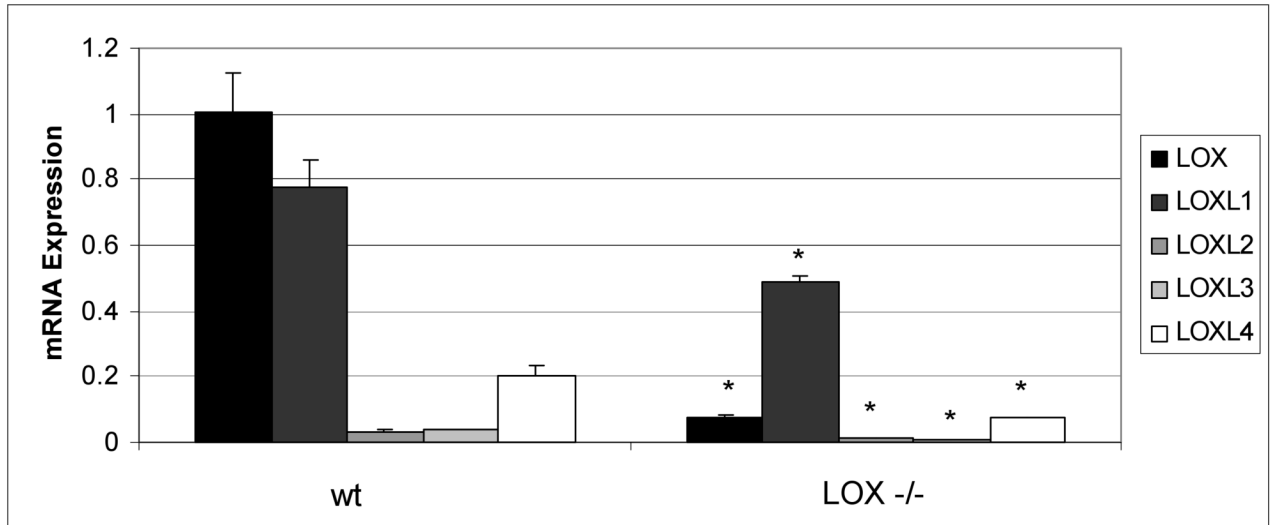


Figure 3. Electronmicroscopic analysis of collagen fibril diameters of craniofacial bone tissues. For each genotype, 500 fibril diameters were measured in randomly chosen areas. Representative images are shown for *Lox*^{-/-} and *wt*. (bar = 30 nm; magnification = $\times 35,000$)

* p < 0.05 compared to wildtype

**Figure 4.**

Real-time RT-PCR analysis of LOX and its isoforms, LOXL1-4, from *Lox*^{-/-} and *wt* mice. Data are presented as mean ± SD obtained from three measurements of pooled RNA samples. Asterisks indicate significant differences between *Lox*^{-/-} and *wt* mice (p < 0.05; unpaired student's *t*-test assuming equal variances).

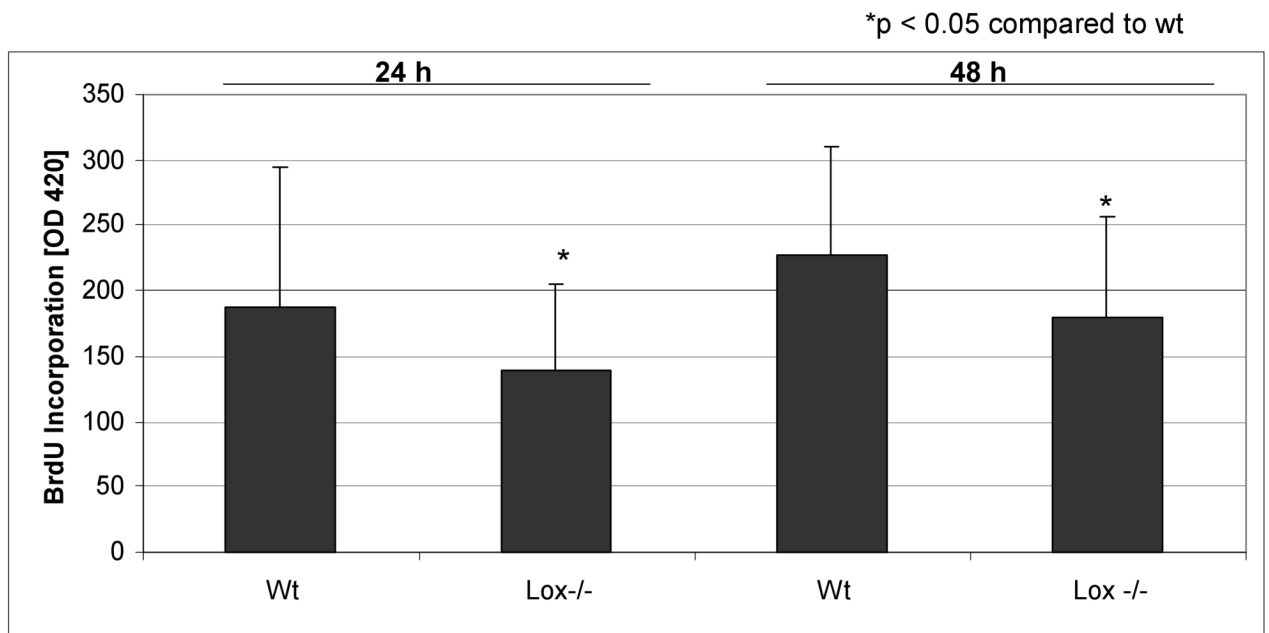
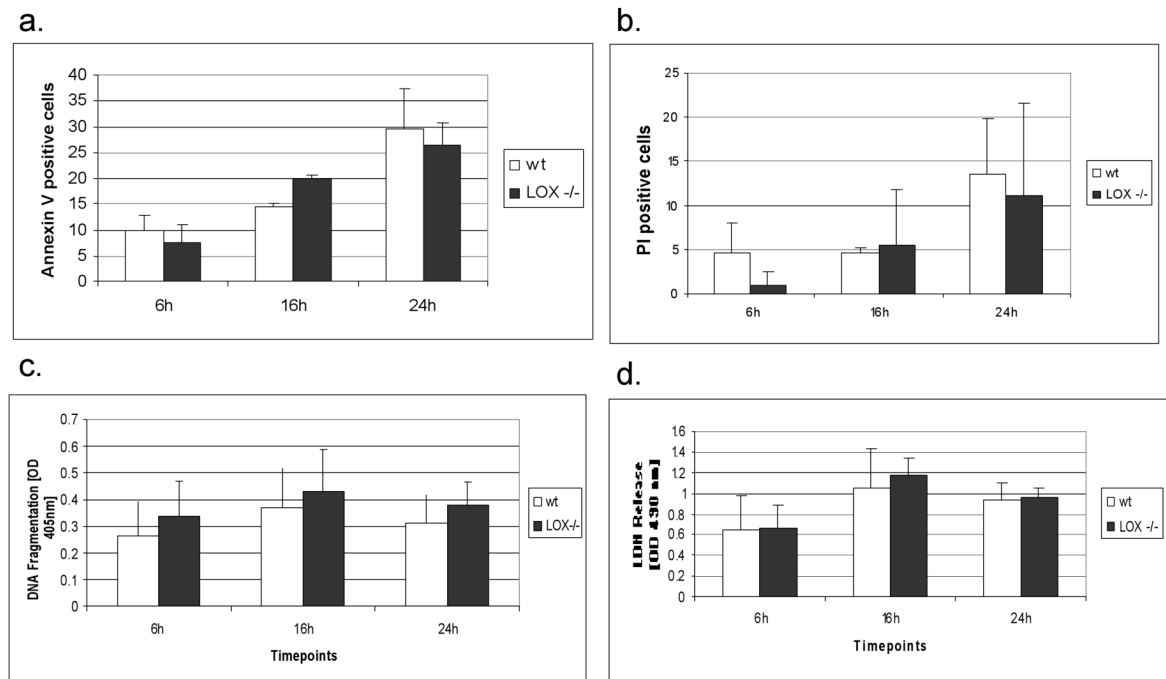


Figure 5.

BrdU incorporation in primary *Lox^{-/-}* and *wt* osteoblastic cells after 24 h and 48 h measured by ELISA at 405 nm. Data are presented as means \pm SD of three experiments ($n = 6$ cultures/genotype). Asterisks indicate significant differences between *Lox^{-/-}* and *wt* cells ($p < 0.05$; unpaired student's *t*-test assuming equal variances).

**Figure 6.**

Annexin-V positive (a), propidium iodine (PI) positive (b) cell count in primary *Lox^{-/-}* and *wt* osteoblastic cells after 6 h, 16 h and 24 h measured by fluorescence microscopy. Measurement of DNA fragmentation (c) in primary *Lox^{-/-}* and *wt* osteoblastic cells after 6 h, 16 h and 24 h by ELISA at 405 nm. Spectrophotometric measurement of LDH release (d) in primary *Lox^{-/-}* and *wt* osteoblastic cells after 6 h, 16 h and 24 h at 490 nm. Data are presented as means \pm SD of three experiments (n = 3 cultures/genotype).

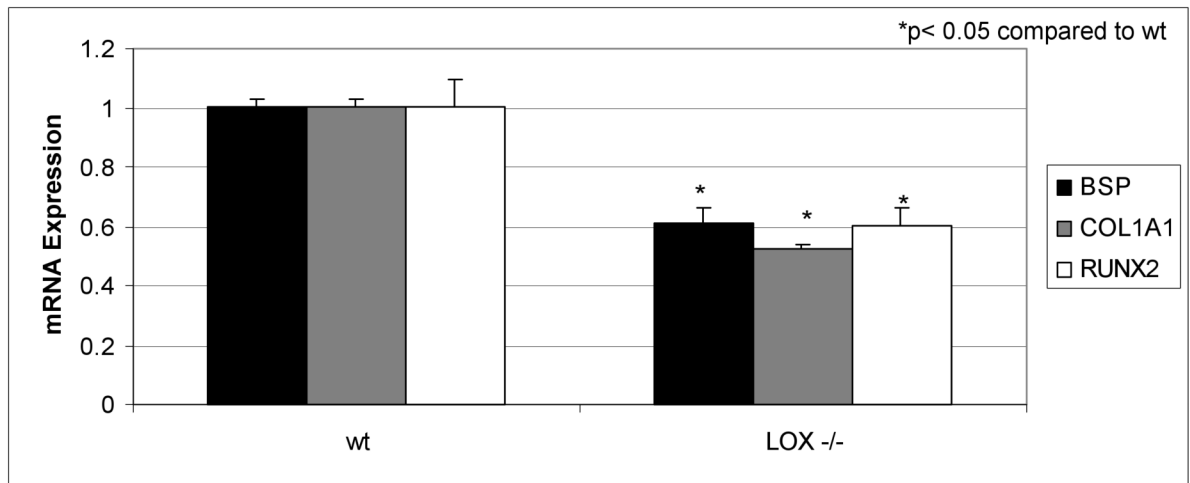


Figure 7.

Real-time RT-PCR analysis of bone markers, COL1A1, bone sialoprotein (BSP) and Runx2/Cbfa1 from *Lox^{-/-}* and *wt* mice. Data are presented as mean \pm SD obtained from three measurements of pooled RNA samples. Asterisks indicate significant differences between *Lox^{-/-}* and *wt* cells ($p < 0.05$; unpaired student's *t*-test assuming equal variances).

Table 1

Means and standard deviations of optical density (OD) of 3 experiments (n = 3 cultures/genotype). Asterisks indicate significant differences between *Lox^{-/-}* and *wt* cells (Alizarin Red eluat of differentiated osteoblasts; p < 0.05; unpaired student's t-test assuming equal variances).

Genotype	Day 14 OD 562 nm [mean ± SD]	Day 21 OD 562 nm [mean ± SD]
<i>Wt</i>	1.156 ± 0.107	1.736 ± 0.134
<i>Lox^{-/-}</i>	0.474 ± 0.066*	0.765 ± 0.087*